Available online at www.sciencedirect.com
ScienceDirect
Trans. Nonferrous Met. Soc. China 25(2015) 3152−3164
Transactions of Nonferrous Metals Society of China
www.tnmsc.cn

Role of nickel alloying on anodic dissolution behavior of zinc in 3.5% NaCl solution. Part II: Potentiodynamic, potentiostatic and galvanostatic studies

Hany M. ABD EL-LATEEF, Abdel-Rahman EL-SAYED, Hossnia S. MOHRAN

Chemistry Department, Faculty of Science, Sohag University, Sohag 82524, Egypt

Received 9 October 2014; accepted 17 March 2015

Abstract: Zinc is common metal used for steel protection from corrosion. The addition of further element, such as Ni, can modify the corrosion rate and maintain sacrificial protection. The anodic dissolution behavior of Zn, Ni and Zn−Ni alloys with different Ni contents (from 0.5% to 10%, mass fraction) in 3.5% NaCl solution was investigated using potentiodynamic, potentiostatic and galvanostatic techniques. The composition and microstructure of the corrosion layer on Zn, Ni and Zn−Ni alloys were characterized by energy-dispersive X-ray spectroscopy analysis (EDX) and scanning electron microscopy (SEM). The galvanostatic curves show that the anodic behavior of all investigated electrodes exhibits active/passive transition and the tendency of the alloys to passivity decreases with the increase in Ni content, except for 99.5Zn−0.5Ni alloy. While the potentiodynamic curves exhibit active passive transition only for pure Zn. Surface analysis reveals the presence of oxides, chlorides and metal hydroxide chloride in corrosion products, and very small cracks are observed for 90Zn−10Ni alloy compared with that of Zn.

Key words: corrosion; NaCl solution; Ni content; Zn−Ni alloy; anodic behavior

1 Introduction

In general, zinc and zinc alloys electrodeposited on steel are of interest due to the improved corrosion protection [1]. However, Zn−Ni and Zn−Co coatings have received more attention than Zn coatings because of their higher degree of corrosion resistance to NaCl in the atmospheric environments [2−5]. Furthermore, BALDWIN et al [6], LIN et al [7] and HEYDARZADEH and JALALI [8] noted that Zn−Ni alloy electrodeposits have better corrosion resistance to NaCl in the atmospheric environment. In addition, RAMANUSKAS et al [9] found that, the mass losses for pure Zn coatings and Zn−Ni coatings were 9 and 5 g/(m^2·year), respectively, whereas in another test site, they were found to be 12 and 6 g/(m^2·year), respectively.

Electrodeposited Zn−Ni alloy coatings are mainly utilized to improve the corrosion resistance of automobile steel bodies [10−13]. However, they also have been used in the applications such as electrocatalytic water electrolysis and electronic industries. In addition, due to their better mechanical properties, they are considered for plating aircraft components [14−16].

MOUNGA et al [17] characterized the corrosion layer formed on zinc exposed to NaCl media. They observed that, this layer was composed of ZnO, $Zn(OH)_2$ and zinc hydroxide chloride or simonkolleite, $Zn_5(OH)_8Cl_2·2H_2O$. The zinc hydroxide chloride and zinc oxide are the dominant corrosion products [1]. While, KALINASUSKAS et al [16] noticed the presence of zinc hydroxide carbonate or hydrozincite ($Zn_5(OH)_6(CO_3)_2·H_2O$) during the exposure in NaCl. However, the hydrozincite layer can be considered as porous layer, accordingly, the passive region is not observed during anodic polarization experiments conducted in an aerated NaCl solution [7].

In spite of the presence of so many publications on the conversion behavior of Zn−Ni alloy electro-deposition in aqueous solutions, there is no work on the corrosion behavior of synthetic Zn−Ni alloys by fusion. Therefore, this work is aimed to show the difference between the electrochemical and corrosion behavior of previous electrodeposited Zn−Ni alloys and those of synthetic alloys by fusion in 3.5% NaCl solution. The

Corresponding author: Hany M. ABD EL-LATEEF; Tel: +20-12-28137103; Fax: +20-93-4601159; E-mail: Hany_shubra@yahoo.co.uk
DOI: 10.1016/S1003-6326(15)63946-2

effect of Ni content on the anodic polarization of Zn−Ni alloys in 3.5% NaCl solution at different temperatures using potentiodynamic, potentiostatic and galvanostatic techniques was studied. The corrosion layers formed on both Zn and its alloy surfaces under different anodic polarization potentials in the examined solution were characterized using energy-dispersive X-ray spectroscopy analysis (EDX) and scanning electron microscope (SEM).

2 Experimental

2.1 Materials and solutions

The solution (3.5% NaCl) was prepared using chemical grade sodium chloride and bidistilled water. The alloys used in this work were prepared by fusion metallurgy at 1000 °C for 24 h. The melts were shaken every 6 h to ensure the homogeneity of melting alloys and finally quenched in ice as previously discussed [18]. Four Zn−Ni alloys were prepared with the compositions of 99.5Zn−0.5Ni (Alloy I), 98Zn−2Ni (Alloy II), 95Zn−5Ni (Alloy III) and 90Zn−10Ni (Alloy IV). The microstructure and composition of the investigated alloys have been mentioned in our previous works [19,20].

2.2 Electrochemical measurements

The measurements were performed on planar disk electrode embedded in an Araldite holder. Before each experiment, the surfaces of the working electrodes were polished using polishing cloth (polishing machine; Buehler, Lake Bluff, Illinois, USA), until their surfaces became smooth and mirror like bright, then degreased in pure ethanol and washed in running bidistilled water before being inserted in the polarization cell. The reference electrode is a saturated calomel electrode (SCE) to which all potentials are referred.

The cell description is given elsewhere [21]. To remove any surface contamination and air formed oxide, the working electrode was kept at −1.50 V (vs SCE) for 5 min in the tested solution, disconnected, shaken free of adsorbed hydrogen bubbles and anodic polarization was recorded. Potentiostat/galvanostat (EG&G Model 273) connected with a personal computer (IBM Model 30) was used for the measurements.

2.2.1 Potentiodynamic technique

The potentiodynamic polarization studies were carried out with electrodes having a surface area of 0.196 cm^2. The potential was altered automatically from the steady state open circuit potential (φ_{corr}) up to −0.775, +1.775 and 0 V (vs SCE) in the case of Zn, Ni and Zn−Ni alloys, respectively and at a scan rate of 1 mV/s using software version 342C supplied from EG&G Princeton Applied Research.

2.2.2 Potentiostatic technique

The anodic potential was fixed at a required constant value and the variation of current density was recorded as a function of time (current density−time transients).

2.2.3 Galvanostatic technique

In this series of experiments, the required anodic current density was imposed on Zn, Ni and Zn−Ni alloys and the variation in anodic potential was measured as a function of time. The current density was measured using the apparent surface area of anode.

2.3 Surface characterization

The composition and morphology of corrosion products formed on the surfaces of the electrodes were examined using energy-dispersive X-ray spectroscopy analysis (EDX) conducted with scanning electron microscope (SEM, JEOL, model 5300).

Each experiment was performed with freshly prepared solutions and clean set of electrodes. Measurements were conducted at 25, 35, 45 and 55 °C for each investigated electrode. For this purpose, ultrathermostat model Frigiter 6000 382 (SELECTA) was used.

3 Results and discussion

3.1 Potentiodynamic polarization measurements

Figure 1 shows the potentiodynamic polarization curves for zinc anode in 3.5% NaCl solution at different temperatures (25−55 °C) in the potential range from −1200 to −750 mV (vs SCE) at a scan rate 1 mV/s. Each anodic curve exihibits two dissolution peaks and a permanent passive region prior to oxygen evolution.

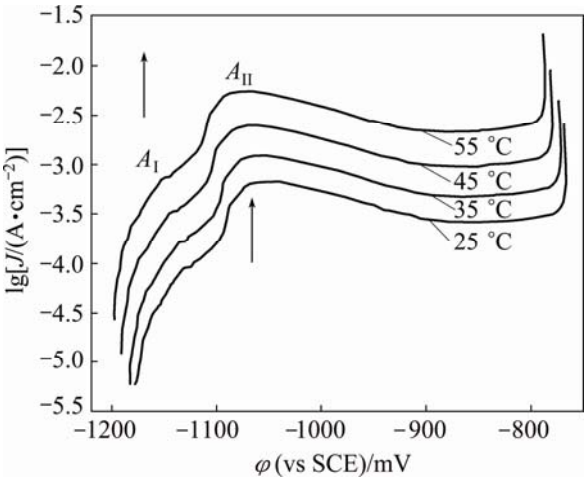

Fig. 1 Potentiodynamic polarization curves for pure Zn in 3.5% NaCl solution at different temperatures

The small peak A_I is defined at about −1.156 V (vs SCE) which can be associated with the active dissolution of Zn to Zn(II) species as previously reported [19,22].

Since the solubility product K_{sp} of zinc hydroxide is markedly low, 3×10^{-17} [23], zinc hydroxide precipitates on the surface of zinc substrate and changes gradually to zinc oxide (peak A_{II}),

$$Zn^{2+}+2OH^{-}\longrightarrow Zn(OH)_2 \quad (1)$$

$$Zn(OH)_2\longrightarrow ZnO+H_2O \quad (2)$$

Consequently, a passive film is formed to prevent zinc corrosion [24]. When chloride ion in the solution reacts with the hydroxide to form soluble Zn^{2+}−Cl^{-}−OH^{-} complex [25], the passive film can be broken down and accelerate local dissolution of zinc, resulting in pitting corrosion [26,27]. However, a protective layer of $Zn(OH)_2$, acting as a barrier to oxygen diffusion, reduces the probability of pitting corrosion.

The anodic current of peak A_{II} is indicative of two processes, the dissolution of the metal and formation of unstable $Zn(OH)_2$ hydroxide converted to ZnO solid phase on the electrode surface. When the electrode surface is completely covered with ZnO film, the dissolution current density falls to a small passive current density (J_{pass}), indicating the onset of passivation. However, when the anodic potential exceeds a certain value, the current rises suddenly to a very high value, suggesting breakdown of the passive oxide film. The potential at which the sudden rise takes place is known as the breakdown potential (φ_b). Crack attack was observed under the scanning electron microscope at −0.789 V (vs SCE).

The passivity breakdown of ZnO film could be ascribed to the ability of Cl^{-} anions to adsorb on the passive film. The adsorbed anions create an electric field across the film/electrolyte interface [28]. When the field reaches a certain value, the adsorbed anions succeed to incorporate and penetrate the oxide film at local defect points. Thus, the kinetics of the reaction is controlled by diffusion of Cl^{-} ions toward the reaction sites, and the oxidation products away from the reaction sites through cracks in the passive film [29]. Consequently, when the penetrated Cl^{-} ions reach the metal substrate, they promote local anodic dissolution, involving the formation of soluble $ZnCl_2$ and the cracks. This indicates the migration of Cl^{-} ions to anodic sites, where zinc hydroxide chloride is formed according to [29,30]:

$$5Zn(OH)_2+2Cl^{-}+H_2O\longrightarrow Zn_5(OH)_8Cl_2\cdot H_2O+2OH^{-} \quad (3)$$

Also, the formation of zinc hydroxide and zinc chloride on the electrode surface may be reacted together to form zinc hydroxychloride as follows:

$$4Zn(OH)_2+ZnCl_2\longrightarrow Zn_5(OH)_8Cl_2 \quad (4)$$

The adsorption and incorporation of Cl^{-} ions into the passive oxide film were supported by the EDX examination of the electrode surface.

It is obvious from Fig. 1 that an increase in temperature increases the anodic peak height (J_p) and shifts its peak potential (φ_p) towards more negative values. These results demonstrate that the temperature increase promotes both the active anodic dissolution and local corrosion of Zn in chloride solution. Figure 2 illustrates the linear relationship between φ_b and temperature, with a temperature coefficient of approximately −0.0008 V/K. The promoting effect of temperature on the local corrosion of Zn may be concerned with two effects: 1) an acceleration in the rates of migration and diffusion of the reactant and product species into and from active sites on the surface and 2) an enhancement in the solubility of ZnO passive film [28].

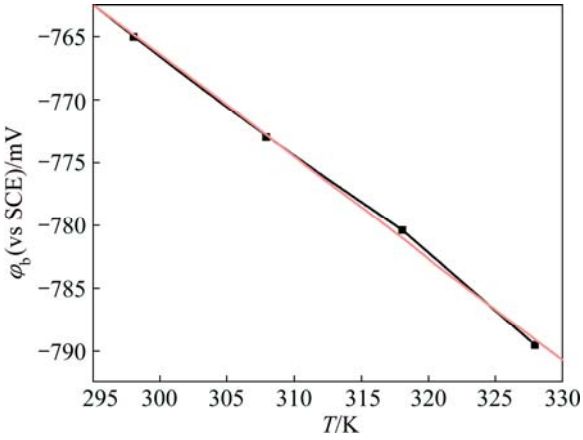

Fig. 2 Dependence of breakdown potential (φ_b) on temperature for pure Zn in 3.5% NaCl solution

Figure 3 shows the potentiodynamic anodic polarization curves of the Ni electrode in 3.5% NaCl solution at different temperatures (25−55 °C). The polarization curves were swept from steady state of open circuit potential (φ_{corr}) up to 2.0 V (vs SCE). The data reveal that the anodic polarization curves exhibit active dissolution. It is seen that Ni has virtually no passive range. The active dissolution extends to 0.1 V, and no passivation of Ni is observed. It is initiated at −0.3 V where a transition region, before the active metal dissolution, is recorded. This region is probably due to the formation of adsorbed species such as $Ni(H_2O)_{ads}$ and/or $NiClOH_{ads}^{-}$ on the electrode surface via the following reactions [31,32]:

$$Ni+H_2O\longrightarrow Ni(H_2O)_{ads} \quad (5)$$

$$Ni+H_2O+Cl^{-}\longrightarrow NiClOH_{ads}^{-}+H^{+}+e \quad (6)$$

In the active region, the anodic current density increases with increasing potential due to the dissolution of the adsorbed species according to the following reactions:

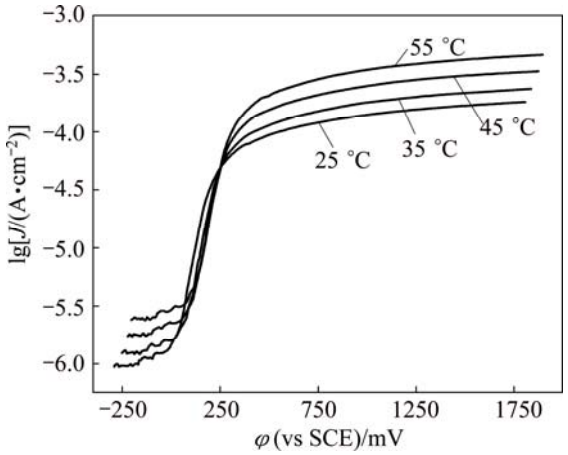

Fig. 3 Potentiodynamic polarization curves for pure Ni in 3.5% NaCl solution at different temperatures

$$Ni(H_2O)_{ads}+2Cl^- \longrightarrow NiCl_2+H_2O+2e \quad (7)$$

$$NiClOH_{ads}^-+Cl^- \longrightarrow NiCl_2+OH^-+e \quad (8)$$

The dissolution of the intermediate species produces new active sites on the electrode surface, and the formation of the passive film is hindered, leading to localized corrosion [33]. Equations (7) and (8) indicate that, the presence of Cl^- increases the solubility of Ni through the probable formation of species such as $NiCl_2$ and/or $NiClOH_{ads}^-$. The effect of temperature on the anodic polarization of Ni in 3.5% NaCl solutions was further investigated. The anodic polarization curves are shifted into the more active direction with increasing the temperature. This indicates that the rise in temperature enhances the anodic dissolution of the nickel.

Figure 4 shows the potentiodynamic J−φ curves of Zn−Ni Alloy IV (as a representative alloy) in 3.5% NaCl solution at different temperatures and a scan rate 1 mV/s. The curves were swept from φ_{corr} up to positive potential (+200 mV (vs SCE)). The data showed that, the active dissolution was initiated at −1.2 V. It is observed that, the curve has two regions. The first one is active dissolution region (from point *A* to point *B*) of 90Zn−10Ni alloy, and dissolution continues with the shift potential to more positive direction until a corrosion layer forms and covers the surface. In this region, zinc in the alloy firstly dissolves as $[Zn(OH)_4]^{2-}$ ions as follows:

$$Zn+4OH^- \longrightarrow [Zn(OH)_4]^{2-}+2e \quad (9)$$

From the point *B* to point *C* (second stage), the alloy dissolution continues gradually, leading to the formation of $Zn(OH)_2$ and/or ZnO at the same time. During the positive polarization of alloy in NaCl solution, the formation of $NiCl_2$ and/or $NiClOH_{ads}^-$ occurs, corresponding to the reactions in Eqs. (5)−(8), respectively. It is evident that in this electrolyte, a passive layer does not form, but a pseudo-passive layer forms. In addition, the alloy surface is gradually covered by the corrosion layer and at point *C*, the corrosion layer confirms the hypothesis of a continuous dissolution of alloy in NaCl solution. According to these results, the layer which is formed on the 90Zn−10Ni alloy surface in a 3.5% NaCl solution is not passive even composed of a mixture of several salts. This layer is porous and much hydrated, it is a pseudo-passive layer.

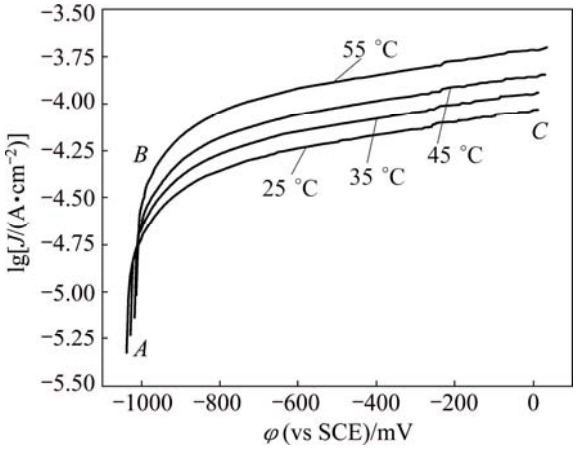

Fig. 4 Potentiodynamic polarization curves for Alloy IV in 3.5% NaCl solution at different temperatures

According to our previous work [19], it is assumed that the addition of Ni to Zn as alloying element decreases the active sites on the alloy surface compared with that of zinc, and the amount of these active sites decreases with increasing Ni content. This behavior can be interpreted on the bases that the increasing γ-Zn_3Ni phase (Alloys I and II) or γ-Zn_3Ni phase with γ-ZnNi (Alloys III and IV) leads to an increase in the corrosion resistance, consequently, and the dissolution rate on the alloy surface decreases. This indicates that the presence of Ni in the alloy plays an important role in significantly reducing the corrosion rate of Zn by increasing the corrosion resistance for the alloy compared to the base metal.

By comparison between the anodic behavior of Zn and that of the investigated alloys, it is observed that the cracks seem to not be formed on the surface of alloy and the current in the pseudo-passive range for Zn−Ni alloys is significantly lower than that of Zn. This behavior can be attributed to the presence of Ni in the alloy composition which can prevent $Zn(OH)_2$ from changing into ZnO. As the Ni content increases, Ni segregates $Zn(OH)_2$ barrier layer via solid-state reaction and incorporates into the cation vacancies. This incorporation competes with the injection of host Zn cations into the corrosion layer and modifies its cracking resistance, leading to a decrease in the corrosion rate of alloys [34]. Accordingly, the rate of corrosion is delayed and the corrosion resistance of the alloy is increased. In addition,

Ni alloying with Zn plays an important role in stabilization of $Zn(OH)_2$ on the alloy surface. Therefore, it slows down the corrosion rate of Zn−Ni alloy in Cl^- ion solution; hence, the increase of Ni content improves the corrosion resistance of these investigated alloys.

3.2 Galvanostatic measurements

Galvanostatic measurement at an anodic constant current density was utilized to get more information about the anodic behavior of Zn, Ni and their investigated alloys in chloride solution. The galvanostatic anodic polarization of the Zn, Ni and Zn−Ni alloys electrodes in 3.5% NaCl solution at 25 °C using various current densities was studied. Figure 5 shows the anodic potential/time curves recorded in 3.5% NaCl solution for Zn electrode. From the variation of the potential of the Zn anode with time, it can be seen that there is a rapid and almost linear change of potential (Region *A*) due to both the decay of hydrogen over potential and the subsequent charging of the electrical double layer at the metal/solution interface [35−37]. This process occurred over a potential range depending upon the magnitude of the polarization current and solution concentration [36]. When this process comes to an end, the potential of the Zn anode changes more slowly with time, giving rise to a distinct arrest (Region *B*). The arrest in potential, φ_{ar}, may correspond to the formation of $[Zn(OH)_4]^{2-}$. The formation of $[Zn(OH)_4]^{2-}$ may be considered the starting point for the dissolution process. Since the potential at this arrest seems to be constant for a certain time, it is assumed that the dissolution rate of Zn in the form of $[Zn(OH)_4]^{2-}$ continues at a rate equal to the rate of oxide film formation (oxidation of Zn to $Zn(OH)_2$ and/or ZnO). This process continues until the active dissolution of Zn is mainly suppressed. The duration of the passivation time, *t* (the time from the start of the anodic polarization until the oxygen evolution), was found to depend on the imposed current densities, *J*. As can be seen from Fig. 5, at the same NaCl concentration, the duration of the passivation time, *t*, decreases with increasing the imposed current densities.

After the passivation time has elapsed, the anodic potential begins to increase in a linear fashion with time (Region *C* in Fig. 5). At this stage, sufficient oxide has accumulated on the electrode surface and, therefore, the rate of oxide film formation was higher than that of the rate of oxide dissolution [38]. According to AMMAR et al [39], the growth of the oxide continues by ionic conduction. The steady state of potential rise at constant current density, i.e., $(d\varphi/dt)_i$, was previously ascribed to the formation of an amorphous oxide known as the barrier oxide layer under galvanostatic anodic polarization. $(d\varphi/dt)_i$ values were related to the polarizing

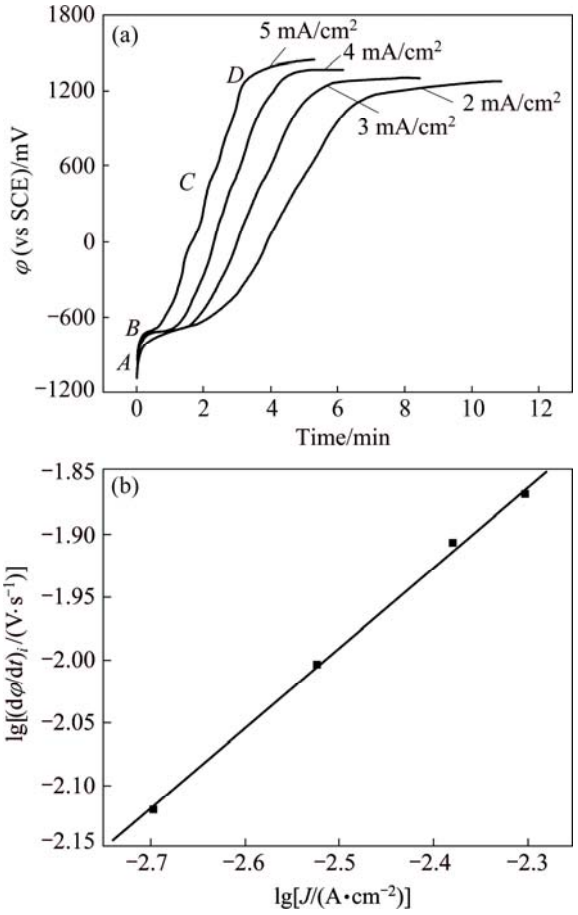

Fig. 5 Anodic potential vs time curves for Zn electrode at different current densities in 3.5% NaCl solution at 25 °C (a) and relation between lg oxide formation rate and lg *J* in same solution (b)

current density, *J*, by the empirical equation [40]:

$$\lg(dE/dt)_i=\lg\ a+b\lg\ J \quad (10)$$

where *a* and *b* are constants characteristics of the metal/solution system [36]. According to Eq. (10), the plot of $(dE/dt)_i$ vs $\lg J$ gives a straight-line relations (Fig. 5(b)). According to AMMAR et al [39], the value of the constant *b* should be 1.0 if the whole applied current density is consumed in oxide formation. The fact that *b* has a value higher than 1.0 indicates that the efficiency of ionic process is slightly lower than 100%. Therefore, a part of ionic current density is consumed in the dissolution process. It is clear from Fig. 5(a) that the rate of oxide film formation increases with increasing imposed current density, *i*. Finally, the polarization curves of Fig. 5 (Region *D*) deviate from linearity to a reach steady state potential value, φ_{st}, which depends upon the concentration of electrolyte and the imposed current density. The potential deviation indicated a decrease in the oxide growth efficiency [36], since at this stage, both oxygen evolution and transformation of $Zn(OH)_2$ to ZnO occurred.

The galvanostatic potential−time curves for Ni electrode in 3.5% NaCl at different current densities ranging from 2 to 5 mA/cm^2 are given in Fig. 6. Careful inspection of these curves indicates that at the beginning of polarization, the anode remains active for a period of time. By tracing the active region, it is noticed that the anode potential rises with time due to oxide growth, and charging curves show two distinct linear regions (*BC* and *CD*). The transition between these two regions, which is accompanied by the appearance of a number of small oxygen bubbles on the surface, is also attributed to structural changes in the anode film. In the active region of Ni, the anode dissolves continuously according to the reaction in Eqs. (5)−(8). The formation of $NiClOH_{ads}^-$ may be considered as the starting point for the dissolution process. Since the potential along this arrest (*AB*) remains constant for a certain time, it is assumed here that the dissolution rate of Ni in the form of $NiClOH_{ads}^-$ continues at a rate equal to the rate of oxide film formation (oxidation of Ni to $NiCl_2$ and/or $NiClOH_{ads}^-$). This process continues until the active dissolution of Ni is mainly suppressed.

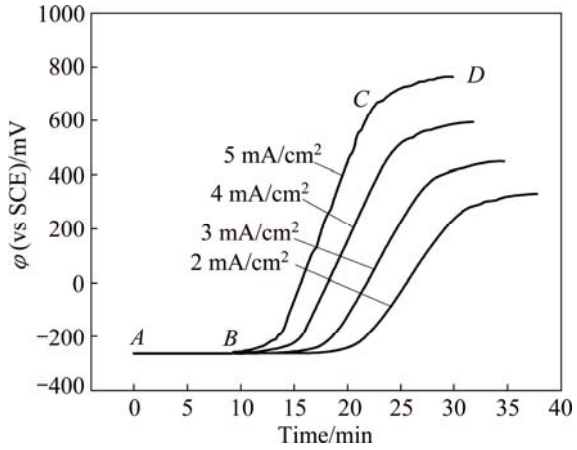

Fig. 6 Anodic potential vs time curves for Ni electrode at different current densities in 3.5% NaCl solution

After the anodic arrest (Region *AB*), the anodic potential begins to increase very rapidly (*BC* region). At this stage, the rate of $NiCl_2$ formation (Reactions (6) and (7)) is higher than the rate of oxide dissolution. Finally, the polarization curves of Fig. 6 (*CD* region) are not deviated from linearity to reach steady state potential value, indicating that the $NiCl_2$ film is more stable on Ni surface. At this stage, both oxygen evolution and transformation of $NiClOH_{ads}^-$ to $NiCl_2$ occur. This behavior is in agreement with the potentiodynamic measurements.

Figure 7 shows the galvanostatic potential−time curves for Zn and Zn−Ni alloys in 3.5% NaCl solution at 2 mA/cm^2. From comparison between these curves, it is observed that the anodic passivation potential of Zn is high compared with that of its investigated alloys under the same conditions. This indicates that, with increasing the percentage of Ni content in the Zn−Ni alloy, the anodic passivation potential values decrease. This behavior confirms that the tendency of the alloy towards passivity decreases as a result of Ni alloying with Zn [37]. This behavior may be due to the stability of the oxide film formed on the alloy surface and higher corrosion resistance. The lower passivation potential of the investigated alloys compared with that of pure Zn can be interpreted on the basis of the competition between the processes occurring on Zn and Ni particles in the alloy. In addition, it may be the presence of Ni with Zn that leads to inhibitive action of Zn oxides on the alloy surface. It is evident that an increase in Ni content in the alloy increases the time needed to achieve passivation (t_{pass}). This indicates that the tendency of alloys to passivity decreases with the increase in Ni content. This behavior can be attributed to the presence of Ni which delays the formation of $Zn(OH)_2$ and/or ZnO on the alloy surface (Zn oxide is formed on the alloy surface before the Ni oxide).

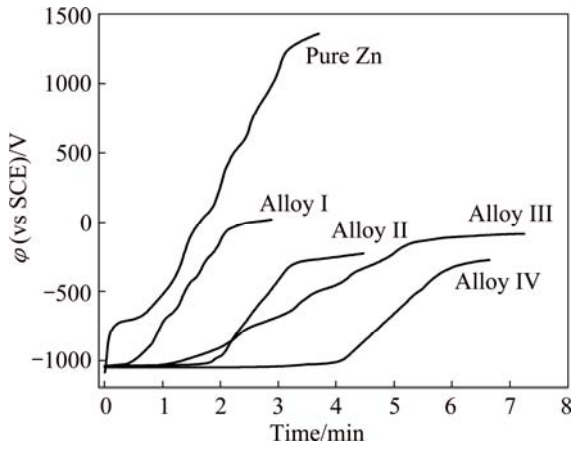

Fig. 7 Comparison between anodic potential vs time curves for pure Zn and Zn−Ni alloys at current density of 2 mA/cm^2 in 3.5% NaCl solution

An increase in the imposed current density, *J*, causes a shift in the starting potential of the arrest, φ_{ar}, into more positive direction according to the following relation [38,40]:

$$\varphi_{ar}=\varphi_{i=0}+ZJ \quad (11)$$

where φ_{ar} is the measured electrode potential at the start of the arrest, $\varphi_{i=0}$ is the potential corresponding to i=0 and Z is a constant. Plots of φ_{ar} vs J in Fig. 8, give a straight line in accordance with Eq. (11). The statistical analysis of the data of Eq. (11) gives a strong correlation coefficient, R^2>0.995 for all investigated electrodes. It is noteworthy to see that, the intersection of these lines with the potential axis gives the value of $\varphi_{i=0}$ equal to

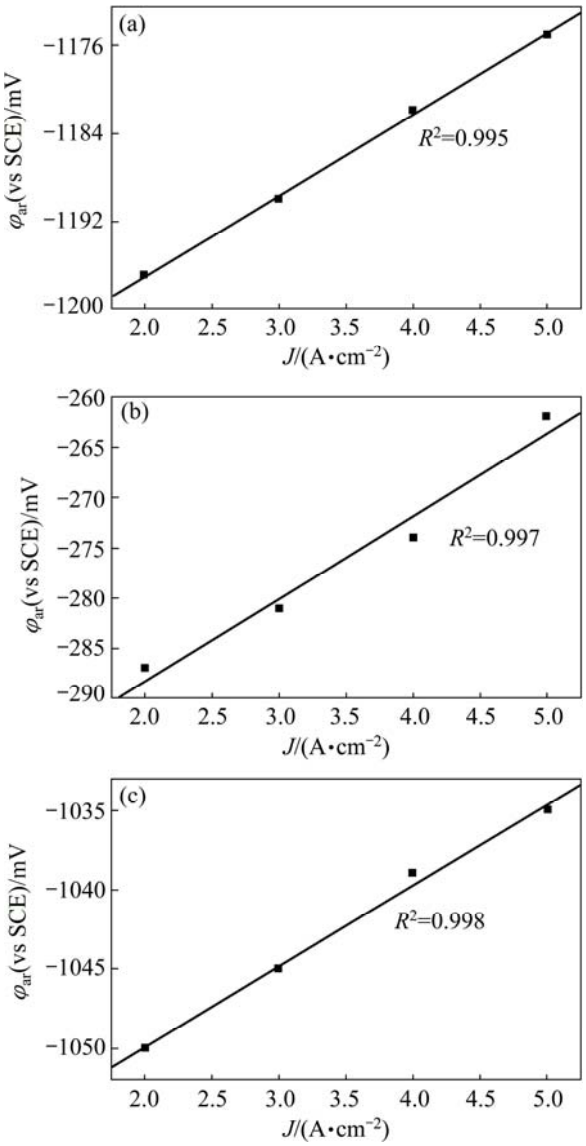

Fig. 8 Variation of starting potential of arrest, φ_{ar}, with current density for pure Zn (a), pure Ni (b) and Alloy IV (c) in 3.5% NaCl solution

−1.198, −0.31 and −1.06 V (vs SCE) for Zn, Ni and Alloy IV, respectively (Fig. 8). It is obvious that the measured arrest potential and the calculated ones for ZnO are nearly similar [41]. Therefore, it may be concluded that, ZnO is formed in this range of potential on the electrode surface and Zn oxide is formed on the alloy surface before the Ni oxide.

The variation of the duration time with the current density on a logarithmic scale is shown in Fig. 9. The data reveal that, as the imposed current density increases, the duration time of the anodic arrest decreases. This behavior may be interpreted on the bases that, the length of the induction period time is limited by the diffusion of Cl^- anions from the bulk of the solution [42]. Thus, at high current density, more Cl^- anions are diffused towards the electrode surface. The variation of duration time of the anodic arrest with Ni content at different current densities is shown in Fig. 10. The data exhibit that, the duration time increases with increasing Ni content from 2% to 10% but decreases for Alloy I (0.5% Ni) and the time required to reach the electrode surface of passivation decreases in the order: Ni > Alloy IV > Alloy III > Alloy II > Zn> Alloy I.

Accordingly, it can be clearly seen that the tendency of the alloys to passivity decreases with the increase in Ni content except for 0.5% Ni. The decrease in the passivation time of Alloy I compared with that of pure Zn may be due to the formation of ZnO and NiO on the alloy surface. So, the oxide blocks the dissolution of active sites and causes inactivation of a part of the surface towards corrosive medium [21]. However, the decrease in steady state of passivation potential of the mentioned alloy may be due to the breakdown of the oxides by Cl^- ions.

3.3 Potentiostatic measurements

The potential range selected for the potentiostatic transients started from −1.075 to +1.0 V (vs SCE), which includes the active and passive zones of the potentio-dynamic curves. Figure 11 shows the current density−time transient curves of Zn electrode in 3.5% NaCl solution at different applied anodic potentials and 25 °C. It is observed that, the current density decreases rapidly with prolonging time to attain a steady state current value. If we neglect the contribution of the double layer charge, the decrease in the transient current may be related to a film growth on the electrode surface. The film growth kinetic fits the model proposed by CHEN et al [43] and MACDONALD and URQUIDI-MACDONALD [44], which is given by

$$J=At^{-n} \tag{12}$$

and/or

$$\lg J=\lg A-n\lg t \tag{13}$$

where A and n are constants depending on the potential limit φ and the electrolyte concentration. The value of n represents the ZnO growth rate [45] and is given by the slope of the descending part of the lg J vs lg t. The data show that, the values of n decrease from 0.349 to 0.121 with increasing applied potential. The values of n show that, the passivation rate increases with the shift of electrode potential towards more positive values. At $\varphi_{applied}$ =−1.075 V (vs SCE), corresponding to peak A_I (Fig. 1), the current density rapidly decreases and attains a steady state value as a result of formation of $Zn(OH)_2$ layer on the electrode surface. Moreover, potentiostatic current−time curves at +1000 mV in 3.5% NaCl solution

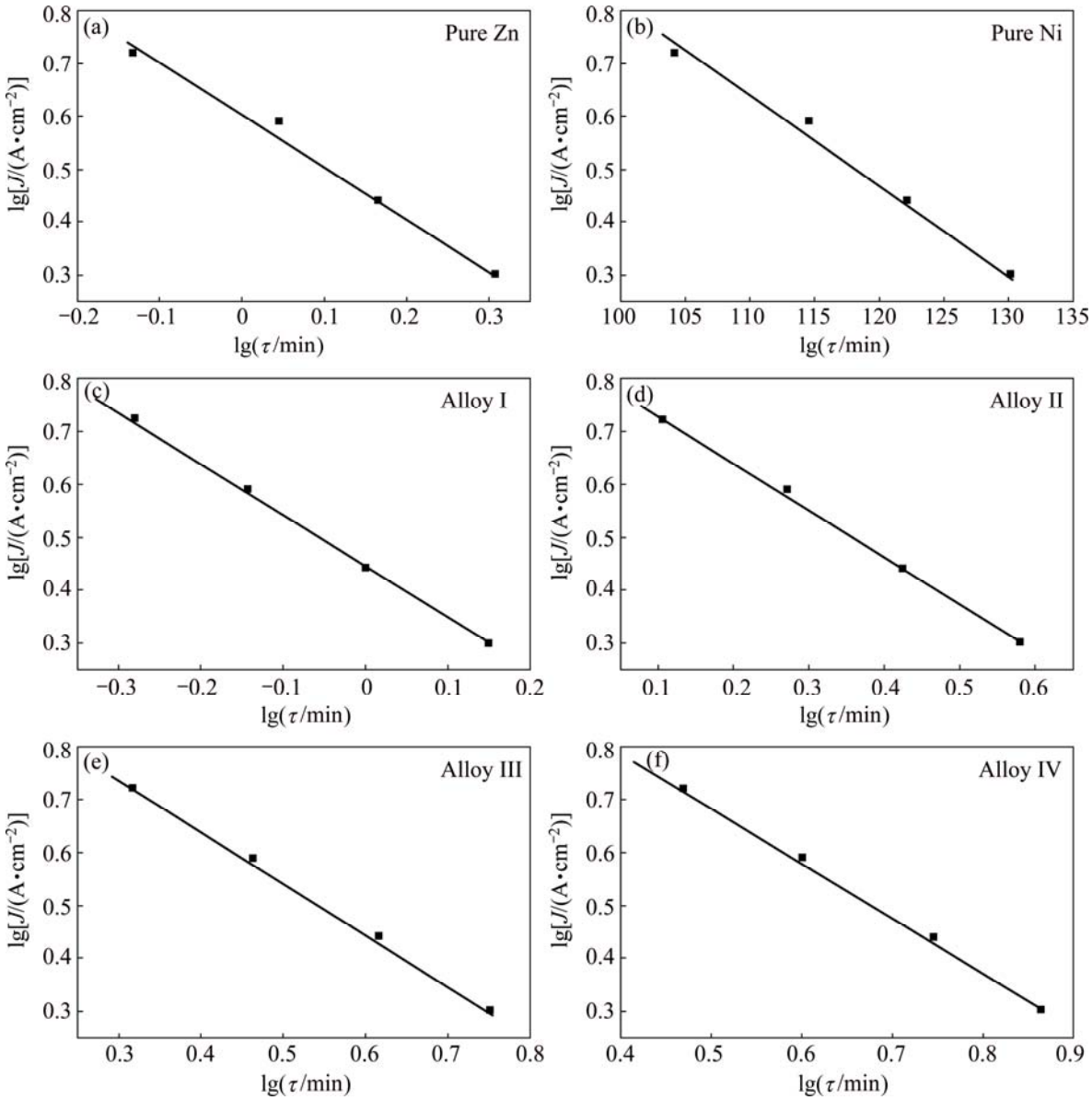

Fig. 9 Variation of duration time of anodic arrest with logarithm of current density for Zn, Ni and Zn−Ni alloys in 3.5% NaCl solution

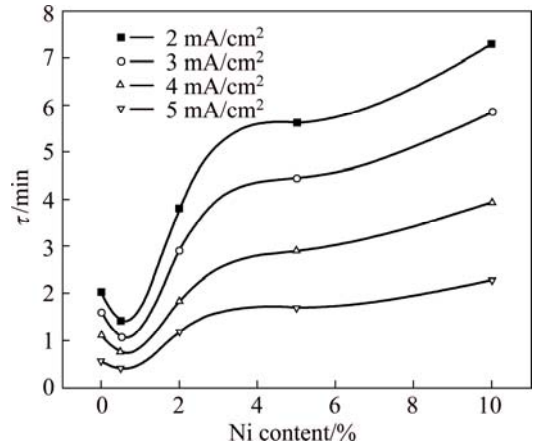

Fig. 10 Variation of duration time of anodic arrest with Ni content at different current densities in 3.5% NaCl solution

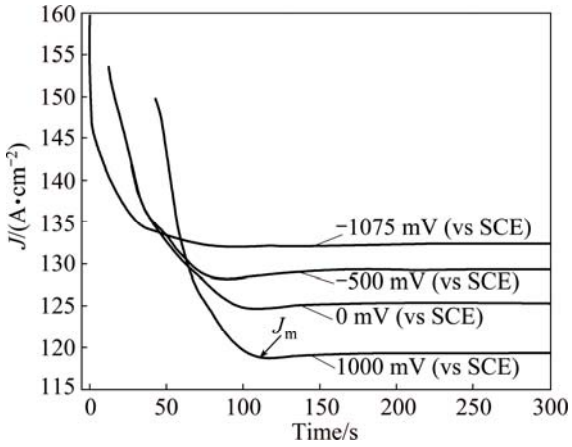

Fig. 11 Potentiostatic transient current vs time curves for pure Zn in 3.5 % NaCl solution at different applied potentials

reveal that, the current density decreases rapidly with the increase of time to a minimum value (J_m).

Figure 12 shows the typical changes of the current density with the increase of time obtained for Ni at various potentials in 3.5% NaCl solution. The current density was observed to decrease with time to attain a steady state current density in the investigated solution. This may be attributed to the formation of a thick barrier layer at more positive applied potential. Current−time transients recorded at different applied potentials for Zn−Ni alloys (Alloy IV as example) in 3.5% NaCl solutions are shown in Fig. 13. Here, it can be seen that, the anodic current density decays in a continuous manner, as the passive film is formed. The results clearly show that the current densities measured for the investigated electrodes in the examined solution at more positive potentials are significantly reduced in comparison with those obtained at more negative potentials. This behavior confirms that the tendency of the investigated electrodes towards passivity increases with shifting applied potential to more positive direction.

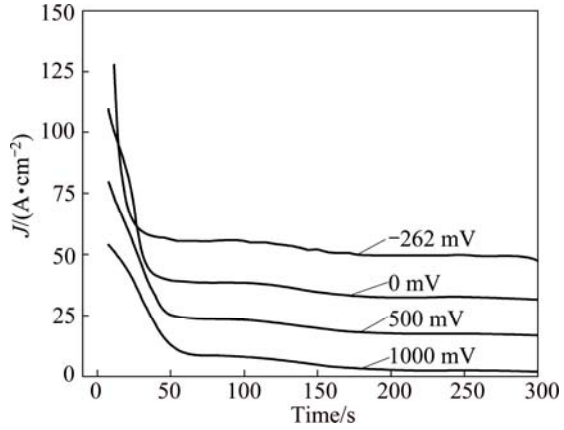

Fig. 12 Potentiostatic transient current density vs time curves for pure Ni in 3.5% NaCl solution at different applied potentials

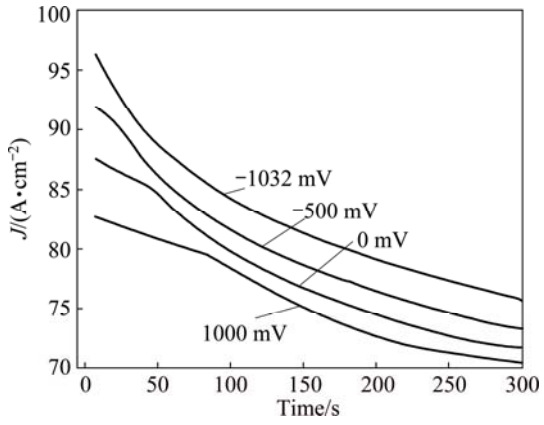

Fig. 13 Potentiostatic transient current density vs time curves for Alloy IV in 3.5% NaCl solution at different applied potentials

3.4 Surface characterization by EDX/SEM analysis

EDX is analytical technique for the elemental analysis or chemical characterization of the corrosion product formed on the electrode surface [46]. EDX analysis revealed the formation of elements O, Na, Cl and Zn on the Zn surface in 3.5% NaCl solution (Fig. 14(a)). Normalized quantitative analysis by stoichiometry, showed that, the surface was covered by NaCl, $ZnCl_2$ and ZnO.

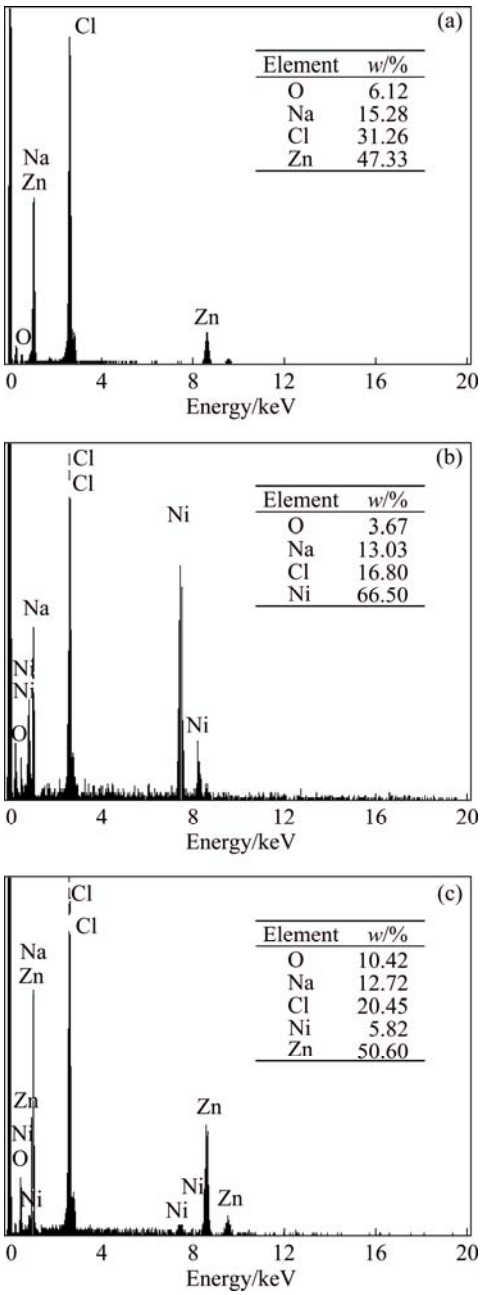

Fig. 14 EDX analysis of corrosion product on Zn electrode (a), Ni electrode (b) and alloy IV (c) surfaces formed anodically in 3.5% NaCl solution

Figure 14(b) shows EDX analysis of the corrosion product on Ni electrode surface formed anodically in 3.5% NaCl solution. The data showed the presence of Ni,

Cl, O and Na. The quantitative analysis confirmed that, the Ni surface was covered with $NiCl_2$ and NiO. Figure 14(c) shows EDX analysis of the corrosion product on Alloy IV surface formed anodically in 3.5% NaCl solution. Analysis of all elements showed the presence of elements Na, Cl, Ni, Zn and O. Analyzed elements combined with Cl and O revealed that the surface of alloy was covered with $ZnCl_2$, $NiCl_2$ and NiO, ZnO_2. This indicated that the pseudo-passivation can be due to the precipitation of the mentioned salts and oxides and/or $NiClOH_{ads}^-$ on the surface.

Figures 15 shows the micrographs of the anodic corrosion film formed anodically on surface of Zn in 3.5% NaCl solution at applied potentials of −1.156 (peak A_I), −1.062 (peak A_{II}), −0.843 and −0.789 V (vs SCE) (dissolution of oxide film). It may appear from Fig. 15(a) that the surface was partially covered by the corrosion product (ZnO) and the electrode surface may be seen. The patches of the corrosion layer exhibited the same shapes. The patches of this layer were not compact, i.e., there were vacancies between them. However, the photograph of Zn treated anodically at −1.062 V (vs SCE) (peak A_{II}), recognized that, the surface was covered by corrosion layer (ZnO and ZnO_2) and the particles were smaller and the amount was greater than that at more negative potential (peak A_I). The patches of this layer were more compact. Figure 15(c) shows the SEM photograph of Zn treated at −0.843 V (vs SCE). It is shown that the surface was almost completely covered by the corrosion layer and the surface contained some cracks. Therefore, SEM results support the potentiodynamic measurements that high current density in the passive region is due to some cracks on the surface. For the electrode surface treated anodically at −0.789 V (vs SCE) (more positive potential, as shown in Fig. 15(d), more cracks appeared in the electrode surface and the amount of corrosion product was decreased compared with that in Fig. 15(c).

Figures 16 shows the micrographs of the corroded surface formed anodically on surface of Alloy IV in 3.5% NaCl solution at applied potentials −0.899 and −0.40 V (vs SCE). It was recognized from Fig. 16(a) that the treated surface at −0.899 V (vs SCE) was partially covered by the corrosion product, so that the electrode surface can be seen. One layer was observed on the electrode surface, and its corrosion product exhibited different shapes compared with that of pure zinc (Fig. 15(c)) and the cracks are not observed. This indicates that the presence of Ni in the alloy as alloying element retarded the anodic dissolution process on the

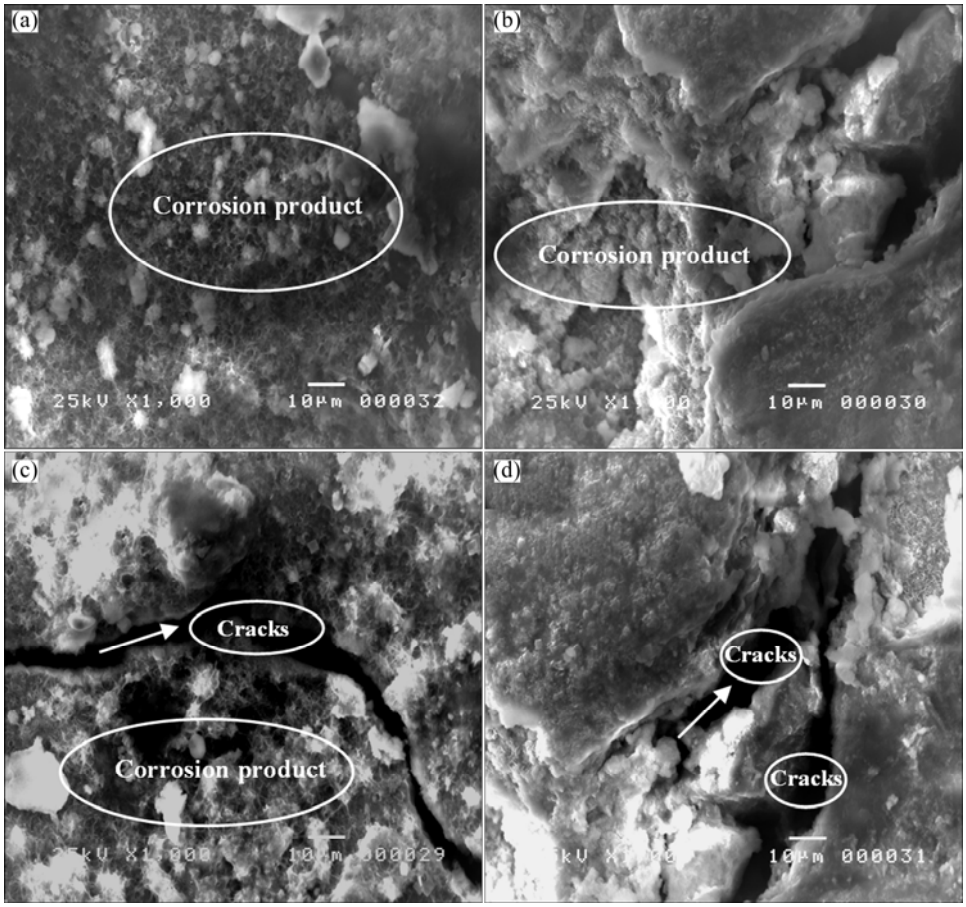

Fig. 15 SEM images of corroded surface of pure Zn formed anodically in 3.5% NaCl solution at −1.156 V (peak A_I) (a), −1.062 V (peak A_{II}) (b), −0.843 V (c) and −0.789 V (cracking) (d)

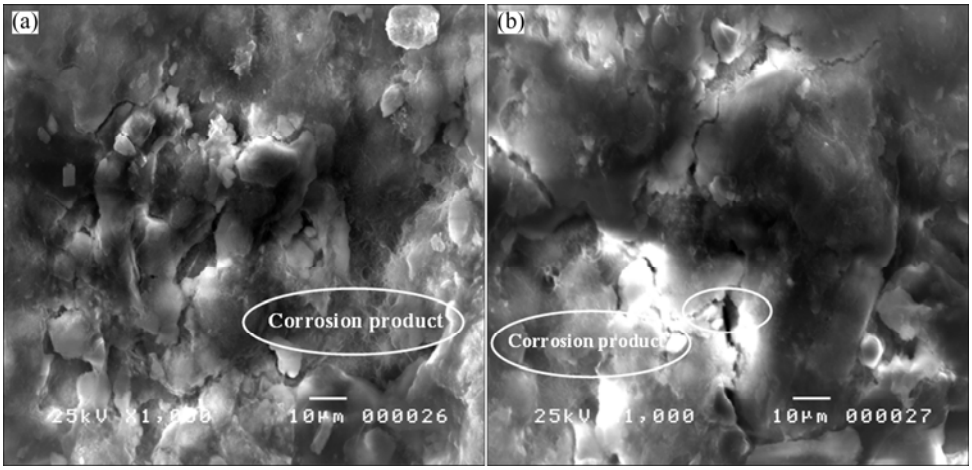

Fig. 16 SEM images of corroded surface of Alloy IV formed anodically in 3.5% NaCl solution at −0.899 V (a) and −0.40 V (b)

alloy surface, and the layer may be related to $Zn(OH)_2$. Figure 16(b) shows SEM photograph of the same alloy treated at −0.40 V (vs SCE). It is found that the surface was covered by adhered thin layer of corrosion product and very small cracks were observed. This result confirms that, the corrosion resistance at more anodic potential of the Zn−Ni alloy was higher than that of Zn.

4 Conclusions

1) Galvanostatic curves show that the anodic behavior of all investigated electrodes exhibits active/passive transition. While the potentiodynamic curves exhibit active/passive transition only in the case of pure Zn. The active dissolution and passive currents increase with increasing temperature.

2) Galvanostatic measurements exhibit that, the passivation time increases with increasing Ni content from 2% to 10%, but decreases for Alloy I (0.5% Ni) and the time required to reach the electrode surface of passivation decreases in the order: Ni > Alloy IV > Alloy III > Alloy II > Zn> Alloy I

3) Potentiostatic measurements reveal that, the current density decreases with the increase of time in the investigated solution. This may be attributed to the formation of a thick barrier layer at more positive applied potential.

4) EDX results indicate that, the passivation can be due to the precipitation of ZnO/ZnO_2 and $ZnCl_2$ on the Zn surface, $NiCl_2$ and NiO on the Ni surface and $ZnCl_2$, $NiCl_2$ and NiO, ZnO_2 on the alloy surface.

5) SEM images exhibit that, the amount of corrosion product increases with shifting the potential to more positive direction, and the cracks are largely observed at more positive potential on Zn surface. However, thin layer of corrosion product with very small cracks is observed for Alloy IV compared with those of Zn under the same conditions. This indicates that, Zn−Ni alloys are more resistive to Cl^- ions attack compared with pure Zn.

References

[1] de ABREU Y, da SILVA A, RUIZ A, REQUIZ R, ANGULO N, ALANIS R. Study of zinc coating on steel substrate attained by tow different technique [J]. Surf Coat Technol, 1999, 120: 682−686.

[2] ASHASSI-SORKHABI H, HAGRAH A, PARVINI-AHMADI N, MANZOORI J. Zinc−nickel alloy coatings electrodeposited from a chloride bath using direct and pulse current [J]. Surf Coat Technol, 2001, 140: 278−283.

[3] FEI Jing-yin, LIANG Guo-zheng, XIN Wen-li. Composition and morphology of Zn−Co alloy coatings deposited by means of pulse plating containing reverse current [J]. Journal of Wuhan University of Technology, 2007, 22: 417−421.

[4] CUNHA A, CARPENTER S D, FERREIRA J Z, CARPENTER D E O S, FARR J P G. Relationship between corrosion resistance, microstructure and cobalt content in a Zn−Co alloy electroplated from alkaline electrolyte [J]. Corrosion Engineering, Science and Technology, 2003, 38(4): 313−316.

[5] GHARAHCHESHMEH M H, SOHI M H. Study of the corrosion behavior of zinc and Zn−Co alloy electrodeposits obtained from alkaline bath using direct current [J]. Mat Chem Phys, 2009, 117(2−3): 414−421.

[6] BALDWIN K R, ROBINSON M J, SMITH C G. Corrosion rate of measurements electrodeposition Zn−Ni alloy coating [J]. Corros Sci, 1994, 36(7): 1515−1526.

[7] LIN Zhi-feng, LI Xiang-bo, XU Li-kun. Electrodeposition and corrosion behavior of zinc-nickel films obtained from acid solutions: Effects of TEOS as additive [J]. Int J Electrochem Sci, 2012, 7: 12507−12517.

[8] HEYDARZADEH SOHI M, JALALI M. Study of the corrosion properties of zinc−nickel alloy electrodeposits before and after chromating [J]. J Mater Process Technol, 2003, 138: 63−66.

[9] RAMANAUSKAS R, MULESHKOVA L, MALDONADO L, DOBROVOLSKIS P. Characterization of the corrosion behavior of Zn and Zn alloy electrodeposits: Atmospheric and accelerated tests [J]. Corros Sci, 1998, 40: 401−410.

[10] FABRI MIRANDA F J, MARGARIT I C P, MATTOS O R, BARCIA O E, WIART R. Corrosion behavior of zinc−nickel alloy electrodeposited coatings [J]. Corrosion, 1999, 55: 732−742.

[11] RAHMAN M J, SEN S R, MONIRUZZAMAN M. Morphology and properties of electrodeposited Zn−Ni alloy coatings on mild steel [J]. J Mechan Engin, 2009, 40: 9−14.

[12] CONCEIÇÃO A M D, JOSÉ W J S, ROBERTO Z N. Corrosion resistance of Zn and Zn−Ni electrodeposits: Morphological characterization and phases identification [J]. Mater Sci Appl, 2013, 4: 644−648.

[13] MOHAN S, RAVINDRAN V, SUBRAMANIAN B, SARAVANAN G. Electrodeposition of zinc–nickel alloy by pulse plating using non-cyanide bath [J]. Transactions of the Institute of Metal Finishing, 2009, 87(2): 85−89.

[14] MOUANGA M, RICQ L, DOUGLADE G, DOUGLADE J, BERÇOT P. Influence of coumarin on zinc electrodeposition [J]. Surf Coat Technol, 2006, 201: 762−767.

[15] QU Q, LI L, BAI W, YAN C, CAO C N. Effects of NaCl and NH_4Cl on the initial atmospheric corrosion of zinc [J]. Corros Sci, 2005, 47: 2832−2840.

[16] KALINAUSKAS P, VALSIUNAS I, SAMULEVICIENE M, JUZELIUNAS E. Zinc photo-corrosion in neutral solutions [J]. Corros Sci, 2001, 43: 2083−2092.

[17] MOUANGA M, RICQ L, DOUGLADE J, BERÇOT P. Effects of some additives on the corrosion behavior and preferred orientations of zinc obtained by continuous current deposition [J]. J Appl Electrochim, 2007, 37: 283−289.

[18] EL-SAYED A, SHAKER A M, EL-KAREEM H G. Anodic behavior of antimony and antimony−tin alloys in alkaline solutions [J]. Bull Chem Soc Jpn, 2003, 76: 1527−1535.

[19] EL-SAYED A, MOHRAN H S, ABD EL-LATEEF H M. Corrosion study of zinc, nickel and zinc-nickel alloys in alkaline solutions by Tafel plot and impedance techniques [J]. Metallurgical Material Transaction A, 2011, 43: 619−632.

[20] ABD EL-LATEEF H M, EL-SAYED A, MOHRAN H S. Role of nickel content in improvement of corrosion resistance of zinc-nickel alloy in 3.5% NaCl solution. Part I: Polarization and impedance studies [J]. Transactions of Nonferrous Metals Society of China, 2015, 25(8): 2807−2816.

[21] ABD EL REHIM S S, HASSAN H H, MOHAMED N F. Anodic behavior of tin in maleic acid solution and the effect of some inorganic inhibitors [J]. Corros Sci, 2004, 46: 1071−1082.

[22] ARAMAKI K. The inhibition effects of chromate-free, anion inhibitors on corrosion of zinc in aerated 0.5 M NaCl [J]. Corros Sci, 2000, 43: 591−604.

[23] LIDE D R. CRC handbook of chemistry and physics [M]. 80th ed. Boca Raton: CRC Press, 1999: 8−111.

[24] D'ALKAINE C V, BOUCHERIT M N. Potentiostatic growth of ZnO on Zn: Application of an ohmic model [J]. J Electrochim Soc, 1997, 144: 3331−3336.

[25] PEULON S, LINCOT D. Mechanistic study of cathodic electrodeposition of zinc oxide and zinc hydroxychloride films from oxygenated aqueous zinc chloride solutions [J]. J Electrochem Soc, 1998, 145: 864−874.

[26] ABD EL-AAL E E. On the pitting corrosion currents of zinc by chloride anions [J]. Corro Sci, 2004, 46: 37−49.

[27] COLE I S, GANTHER W D, FURMAN S A, MUSTER T H, NEUFELD A K. Pitting of zinc: Observations on atmospheric corrosion in tropical countries [J]. Corro Sci, 2010, 52: 848−858.

[28] MOHAMMED A A, HAMDY H H, ABD EL REHIM S S. On the role of NO_2^- ions in passivity breakdown of Zn in deaerated neutral sodium nitrite solutions and the effect of some inorganic inhibitors: Potentiodynamic polarization, cyclic voltammetry, SEM and EDX studies [J]. Electrochimica Acta, 2008, 53: 2600−2609.

[29] MOUANGA M, BERCOT P, RAUCH J Y. Comparison of corrosion behavior of zinc in NaCl and NaOH solutions. Part I: Corrosion layer characterization [J]. Corros Sci, 2010, 52: 3984−3992.

[30] MOUANGA M, BERCOT P. Comparison of corrosion behavior of zinc in NaCl and NaOH solutions, Part II: Electrochemical analysis [J]. Corros Sci, 2010, 52: 3993−4000.

[31] ZHANG Zhong-ju, ZHU Yan-juan, BAO Jie, ZHOU Zhuo-jun, YE Xian-cong, XU Qing-shen. Effect of ultrasonic on structure and electrochemical performance of α-$Ni(OH)_2$ electrodes [J]. Transactions of Nonferrous Metals Society of China, 2011, 21(12): 2654−2659.

[32] MUÑOZ A G, SCHULTZE J W. Effects of NO_2^- on the corrosion of Ni in phosphate solutions [J]. Electrochimica Acta, 2004, 49: 293−301.

[33] REN Wen-da, LI Jin-feng, ZHENG Zi-qiao, CHEN Wen-jing. Localized corrosion mechanism associated with precipitates containing Mg in Al alloys [J]. Transactions of Nonferrous Metals Society of China, 2007, 17(4): 727−732.

[34] BADAWYA W A, ISMAILA K M, FATHIB A M. Effect of Ni content on the corrosion behavior of Cu−Ni alloys in neutral chloride solutions [J]. Electrochimica Acta, 2005, 50: 3603−3608.

[35] ABD EL WANEES S, ABD EL AAL MOHAMED A, ABD EL AZEEM M, ABD EL FATAH A N. Pitting corrosion currents of tin in relation to the concentration of the inhibitive and corrosive anions under natural corrosion conditions [J]. Int J Electrochem Sci, 2008, 3: 1005−1015.

[36] ABD EL AAL E E. Kinetic studies of zinc passivation in borate solutions under different conditions [J]. Corrosion, 1999, 55: 582−589.

[37] ABD EL AAL E E. Effect of Cl^- anions on zinc passivity in borate solution [J]. Corros Sci, 2000, 42: 1−16.

[38] ABD EL AAL E E. Studies on the anodic and cathodic polarization of lead in sodium sulphate solution [J]. J Power Sources, 1998, 75: 36−43.

[39] AMMAR I A, DARWISH S, KHALIL W W, EL TAKER S. Galvanic effects on the active dissolution of duplex stainless-steels [J]. Corrosion, 1990, 46: 197−202.

[40] ABD EL AAL E E. Oxide film formation on zinc in borate solutions in open circuit [J]. Corros Sci, 2008, 50: 41−46.

[41] EL-SAYED A, MOHRAN H S, ABD EL-LATEEF H M. Effect of minor nickel alloying with zinc on the electrochemical and corrosion behavior of zinc in alkaline solution [J]. J Power Sources, 2010, 195, 6924−6936.

[42] ABD EL AAL E E. Passivity and passivity breakdown of zinc anode in sulphate solutions [J]. Anti-Corros, 1999, 46: 349−357.

[43] CHEN Y, LOBO R F M, SANTOS D M F, SEQUEIRA C A C. Kinetic measurements during transient film growth on zinc [J]. Quím Nova, 2009, 32: 387−390.

[44] MACDONALD D D, URQUIDI-MACDONALD M. Theory of steady state passive films [J]. J Electrochim Soc, 1990, 137: 2395−2402.

[45] HASSAN H H. Corrosion behavior of zinc in sodium perchlorate solutions [J]. Appl Surf Sci, 2001, 174: 201−209.

[46] FIGUEROA G, VALENZUELA J L, PARGA J R, VAZQUEZ V, VALENZUELA A. Recovery of gold and silver and removal of copper, zinc and lead ions in pregnant and barren cyanide solutions [J]. Mater Sci Appl, 2015, 6: 171−182.

Ni 合金化对 Zn 在 3.5%NaCl 溶液中阳极溶解行为的影响(II): 动电位、恒电位和恒电流研究

Hany M. ABD EL-LATEEF, Abdel-Rahman EL-SAYED, Hossnia S. MOHRAN

Chemistry Department, Faculty of Science, Sohag University, Sohag 82524, Egypt

摘　要：Zn 是钢防腐常用的金属。进一步添加其他元素，如 Ni，可以降低其腐蚀速率，保持其牺牲性保护作用。采用动电位、恒电位和恒电流技术研究 Zn、Ni 和不同 Ni 含量(0.5%~10%)的 Zn−Ni 合金在 3.5%NaCl 溶液中的阳极溶解行为。利用 EDX 和 SEM 对 Zn，Ni 和 Zn−Ni 合金腐蚀层的成分和显微组织进行表征。恒电位曲线表明，所有研究电极的阳极行为都呈现活化/钝化转变，而且除 99.5Zn−0.5Ni 合金外，随着 Ni 含量的增加，合金的钝化趋势减弱。而动电位曲线表明，只有 Zn 表现出活化/钝化转变。表面分析表明，腐蚀产物主要为氧化物、氯化物和氢氧氯化物。与 Zn 相比，90Zn−10Ni 合金中可观察到细微的裂纹。

关键词：腐蚀；NaCl 溶液；Ni 含量；Zn−Ni 合金；阳极行为

(Edited by Yun-bin HE)